Generalization and Modelling of Rigid Polyisocyanurate Foam Reaction Kinetics, Structural Units Effect, and Cell Configuration Mechanism

Jie Xu[1], Tao Wu[1,], Wei Sun[2], and Chuang Peng[3,*]*

[1]Department of Chemical and Environmental Engineering, Faculty of Science and Engineering, University of Nottingham Ningbo Campus, Ningbo, China 315100
[2]Department of Mechanical Engineering, Faculty of Engineering, University of Nottingham, Nottingham, UK NG7 2RD
[3]School of Resource and Environment Sciences, Wuhan University, Wuhan, Hubei, China 430079

Received: 22 February 2017, Accepted: 8 May 2017

GRAPHICAL ABSTRACT

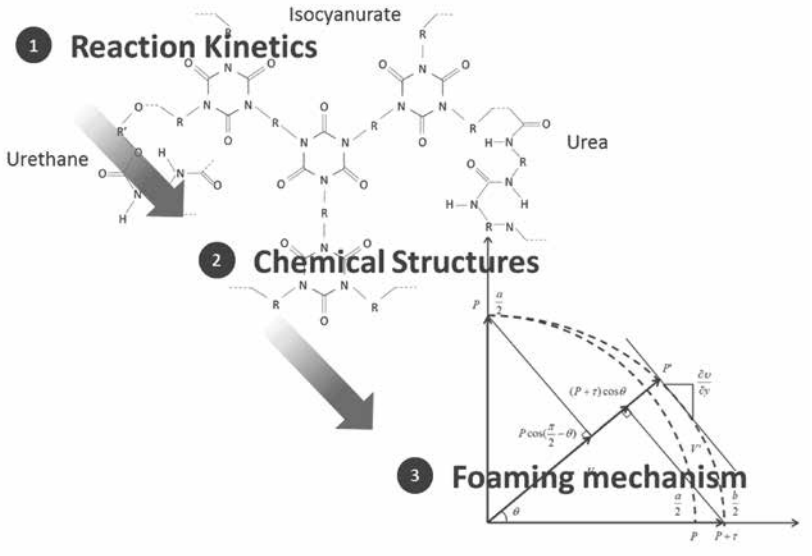

* Corresponding authors. Email: Tao.wu@nottingham.edu.cn (Tao Wu) and Chuang.peng@whu.edu.cn (Chuang Peng)

SUMMARY

PIR/PUR ratio was derived from differential manipulation of generalized polyisocyanurate kinetic model. The structural unit effects on polymerization of isocyanurate, urethane and urea linkages were evaluated based on Mayo-Lewise tercopolymerization scheme. The cell microstructural configuration model was further developed from profiled FOAMAT reactivity parameters with integrated analysis of cell interface physics. The interstitial border area was defined by interface free energy theory, the shear viscosity was evaluated by foam motion, gas fraction, and partial pressure, and the cell inflation was re-examined by gas-liquid surface tension variability. The cell anisotropic degree, assumed as an aspect ratio of infinitesimal volume elements in cell uniformity, was characterized by equilibrated work increase of surface energy approximated by 2D stretching deformation from sphere cell to spheroid cell. The relationship between pressure and surface tension of elongated cells was also derived from modelling at the same condition of cell deformation.

Keywords: Polyisocyanurate, PIR/PUR ratio, Polymerization, Cell interstitial area, Degree of anisotropy

INTRODUCTION

Polyurethane reactions scheme can be generalized as integration of blowing and gelling which includes primary water-hydroxyl-isocyanate reactions and secondary isocyanate oligomerizations. The polycondensation creates linkages of urethane and urea units through chain extension. Carbon dioxide is generated from unstable transition-state carbamic acid [1]. The released heat vaporizes the blowing agents and drives primary reactions further towards secondary crosslinking. This reaction system is usually complicated by reversible side reactions, such as isocyanate-urea reaction forming biuret and urethane-isocyanate reaction forming allophanate. The concentration excess of isocyanate can aggravate self-cycling biuretisation and dimerisation, and meanwhile promote primary isocyanurate trimerisation. The four-membered ring uretidinedione forms by cycloaddition of two C=N bonds [2]. This exothermic dimerization can be broken by heating at ~160ºC and form allophanate with more hydroxyl group presence [3]. Uretidinedione is undesirable and thermally unstable side product and able to further react with isocyanates at very high temperatures and generate carbodiimides. The irreversible carbodiimide formation promotes the formation of reversible trifunctional uretonimines which can increase the crosslink density [4]. A certain degree of isocyanurate unit from isocyanate trimerization can be observed in characteristic polyisocyanurate chain structure which can be characterized mathematically by PIR/PUR ratio [5] based on kinetic reaction evaluation.

Polymerization of polyisocyanurate is quite example of copolymerizations. It can be self-catalyzed by complex association between diols and diisocyanates or additionally catalyzed by alkalinity to avoid undesirable reversible side reactions. This heteropolyaddition is usually manipulated by both hydroxyl and isocyanate functional groups with calculated stoichiometric equivalence. The isocyanates in excess may lead to homocyclization. The urethanization kinetics scheme can be defined as integration of chain growth by A-A and B-B monomers, step growth of polymeric A-$(A)_{n-2}$-A and B-$(B)_{n-2}$-B, chain transfer (branching) of chain extender/crosslinker, and crosslinking of $(AB)_n$. The combination of the amount of polyfunctional monomers polymerization and the extent of biuret, allophanate, and trimerization reactions dictates the sequence distribution. The urethane linkage formation creates alternating order and the urea formation by water leads to tercopolymer. More polyol soft segments result in more block statistics and more isocyanate oligomers can escalate the distribution disorderedness. Meanwhile, overall physical and chemical controls on curing process can complicate the crosslinking polymerization [6, 7].

The polyurethane foaming process has been widely studied. Usually the polymerization models were developed based on progressive monitoring of foaming and curing dynamics and calculating the motion parameters and the rheological flows of filling quality [8-13]. For instance, a one-dimensional model for foam expansion with water and R-11 blowing was developed based on first order reaction kinetics [8]. One foam density prediction was made by residence time approach to understand free rise foams in two-dimensions [9]. Another foam expansion model was developed using finite volume method with a time-dependent density function to successfully predict three-dimensional refrigerator cavity foam growth based on corrected Castro-Mascosko curing viscosity model with dilute assumption [10]. Additionally, Mao foaming model by Eulerian flux-splitting method integrating motion equations and Baser-Khakhar kinetics with a viscosity constant successfully predicted bubble-radius based on gas volume fraction and bubble number density estimation which even further extrapolated the possible filling behavior of a free rise foam, Hele-Shaw flow and complex three-dimensional microgeometry [11]. For more applied industrial research, one thermal kinetics experimentally built foaming-curing model using finite volume discretization in commercial code between the foam and gas was developed to track volume of fluid equation of free-rise foam and refrigerator cavity filling [12]. Another model by three-dimension space-time finite element method with reduced order foaming kinetics in continuity equation [13] based on bubble-scale model was also developed from Piloyan law of curing reaction and Castro-Macosko curing rheology [14] to predict car seat foaming.

The purpose of this study is to provide deep understanding of catalyzed polyisocyanurate reaction kinetics, copolymerization structural units effect, and cell configuration mechanism. The kinetic mathematic manipulations were performed on differential rate equations of simplified polyisocyanurate polymerization schemes in order to derive the kinetic relationship with practical [PIR]/[PUR] ratio. The kinetic schemes were then transferred into generalized Mayo-Lewise tercopolymerization scheme to characterize the isocyanate conversion during urethanization. The structural unit effect of isocyanate in polymerization was analyzed by mole ratio of monomers and unit ratio of urethane/urea. Furthermore, the cell microstructural configuration was studied based on measured foaming parameters from commercially available FOAMAT software. The model was built on interstitial border area analysis of surface tension and Gibbs free energy. The cell orientation was also predicted through 2D geometric cell deformation of assumed elongation.

POLYISOCYANURATION KINETICS

The copolymerization process of polyurethane can be distinguished somehow at gel time when is the time of visible insoluble polymer fraction formation from hydroxyl functional branching and isocyanate oligomer crosslinking. In most cases, polyisocyanurate has more isocyanate oligomers from cyclization and secondary addition which provides more crosslinking points to form chains with unit segments of urethane and urea and more branching points to react with polyfunctional hydroxyl groups. In this study, the sequence arrangements of all compounds were analyzed by polymer statistics (**Table 1**). The kinetic scheme was constructed based on assumption of macroglyol A_f of polyether or polyester and polymeric isocyanate B_f of a complex mixture with pure monomers and higher homologues. The secondary reactions forming isocyanate oligomers and hydroxyl prepolymers are all generalized.

Table 1. Statistical sequence arrangements of polyisocyanurate foam

Chemicals	Sequences
Urethane unit	$A_{(f-1)}\ (AB)_n\ A_{(f-1)}$
Urethane/urea unit	$A_{(f-1)}\ (AB)_n\ (NCN)_n\ A_{(f-1)}$
Allophanate	$B_{(f-1)}\ (AB)_n\ B_{(f-1)}$
Biuret	$B_{(f-1)}\ (NCN)_n\ B_{(f-1)}$
Acylurea	$B_{(f-1)}\ (NC)_n\ B_{(f-1)}$
Polyisocyanurate	$\{A_{(f-1)}\ [(AB)_n;\ (NCN)_n][(AB)_{(f-1)};(NCN)_{(f-1)};\ (NC)_{(f-1)};\ B_{3(f-1)}]\}_n$
Notes: f is termed the functionality of polyols/isocyanates *NCN denotes urea linkage* *NC denotes amide structure*	

Urethanization chemistry entails various isocyanate reactions of self-additions and trans-condensations with corresponding functional linkages generation. The reversible associated isocyanate complex and active hydrogen bond formation proportionally catalyzes the reactions. The recognized polyurethane self-catalyzation resulting from electrophilic-nucleophilic substitution between oxygen and carbon generates isocyanate-hydroxyl complex with hydrogen bonding to isocyanate nitrogen atom. The similar active complex can form in extra catalyzed system. These complexes are reversibly associated with unbounded compounds servicing as an intermediate for subsequent rate-determining urethane conversion. The primary and side reactions in this study are all based on catalyzation steady-state law which approximates the concentration of associated active complex in reactions are pretty low and not changing over time.

Moreover, those copolymerization reactions in **Table 1** were further simplified into reduced cumulative second order elementary reactions which are two deliberately separated equations of both PUR reaction representing urethane/urea chain segments formation and PIR reaction representing isocyanate oligomers formation. Bulk copolymerization as the simplest process was assumed as pre-conditions. The stoichiometric equilibrium was also hypothesized here.

$$ISO((1-p)B_f) \overset{K_i}{\Rightarrow} PIR \tag{1}$$

$$POL\ (A_f) + ISO(pB_f) \overset{K_u}{\Rightarrow} PUR \tag{2}$$

So the differential rate equations can be developed:

$$\frac{d[PIR]}{dt} = K_i[ISO'] \tag{3}$$

$$\frac{d[PUR]}{dt} = K_u[POL][ISO] \tag{4}$$

By solving Eq (3) and Eq (4), [*PIR*] and [*PUR*] can be obtained:

$$[PIR] = (1-p)[ISO]_0(1-e^{-K_i t}) \tag{5}$$

$$[PUR] = [POL]_0\left(1 - e^{-\frac{K_u}{K_i}p[ISO]_0\left(1-e^{-K_i t}\right)}\right) \tag{6}$$

So the isocyanate trimer compound ratio in polyisocyanurate foam (PIR/PUR ratio) becomes:

$$\frac{[PIR]}{[PUR]} = \frac{(1-p)[ISO]_0\left(1-e^{-K_i t}\right)}{[POL]_0\left(1-e^{-\frac{K_u}{K_i}p[ISO]_0\left(1-e^{-K_i t}\right)}\right)} = \frac{1-p}{p}\frac{1-e^{-K_i t}}{1-e^{-\frac{K_u}{K_i}[POL]_0\left(1-e^{-K_i t}\right)}} \tag{7}$$

At steady-state condition, the polyisocyanurate forms when conversion rates of urethane/urea chain segments and isocyanate oligomers crosslinking points reach maximum, when the polyol concentration is close to zero, then $V_{\max(PUR)}$ can be written into:

$$V_{\max\,(PUR)} = K_u(1-p)[ISO]_0 e^{-K_i t} \tag{8}$$

So [*PIR*]/[*PUR*] ratio can be transformed into follows:

$$\frac{[PIR]}{[PUR]} = \frac{V_{\max\,(PIR)}}{V_{\max\,(PUR)}} = \frac{(1-p)[ISO]_0(1-e^{-K_i t})}{K_u(1-p)[ISO]_0 e^{-K_i t}} = \frac{1-e^{-K_i t}}{K_u e^{-K_i t}} \tag{9}$$

COPOLYMERIZATION STRCTUREAL UNITS EFFECTS

Mayo-Lewis Tercopolymerization Modelling

The generalized polyurethanization kinetic scheme was created based on Mayo-Lewise equations. The ternary step polymerization considers one difunctional monomer of isocyanate A-A reacting with two types of hydroxyls both diol and water. Thus two structural units – urethane and urea - forms from two chain growth polyadditions – hydroxyl-isocyanate (A-A and B-B) and water-isocyanate (A-A and C-C). The coordination copolymerization of amine and water were neglected. The reversible isocyanate oligomerizations were not treated but the self-homocyclizations were considered in the scheme. Under steady state approximation, the intermediate amine from water-reaction was set to ineffective zero. Then, the mixing components of A-A, B-B, C-C reacting with reactive chain end terminating in either same group can be interpreted in following scheme:

$$\mathrm{A-A*+A-A} \xrightarrow{\mathrm{k11}} \mathrm{A-(AA)-A^*} \tag{10}$$

$$A-A*+B-B \xrightarrow{k12} A-(AB)-B^* \tag{11}$$

$$A-A*+C-C \xrightarrow{k13} A-(AC)-C^* \tag{12}$$

$$B-B^*+A-A \xrightarrow{k21} B-(BA)-A^* \tag{13}$$

$$C-C^*+A-A \xrightarrow{k31} C-(CA)-A^* \tag{14}$$

Where k_{11} was defined as the generalized rate constant representing isocyante trimerization because the isocyanate self-polymerization can be perceived as homocyclization dominated step growth. k_{ij} denotes the rate constant of heteropolyaddition. The reaction rates of each monomers can be obtained by following equations:

$$-\frac{d[A]}{dt} = k_{11}[A^*][A] + k_{21}[B^*][A] + k_{31}[C^*][A] \tag{15}$$

$$-\frac{d[B]}{dt} = k_{12}[A^*][B] \tag{16}$$

$$-\frac{d[C]}{dt} = k_{13}[A^*][C] \tag{17}$$

Furthermore, define the reactivity ratio as aspect ratio of two rate constants of element equations:

$$r_{a1} = \frac{k_{11}}{k_{11}} = 1 \tag{18}$$

$$r_{a2} = \frac{k_{11}}{k_{12}} \tag{19}$$

$$r_{a3} = \frac{k_{11}}{k_{13}} \tag{20}$$

Then further set f_x as mole fraction of monomer x in the feed at the same instant of time. The composition equation can be derived based on differential evaluations:

$$Y_a = \frac{\frac{d[A]}{dt}}{\frac{d[A]}{dt}+\frac{d[B]}{dt}+\frac{d[C]}{dt}} = \frac{k_{11}[A]+k_{12}[B]+k_{13}[C]}{k_{11}[A]+2(k_{12}[B]+k_{13}[C])} = \frac{\frac{k_{11}}{k_{13}}f_a+\frac{k_{12}k_{11}}{k_{11}k_{13}}f_b+f_c}{\frac{k_{11}}{k_{13}}f_a+2\left(\frac{k_{12}k_{11}}{k_{11}k_{13}}f_b+f_c\right)} =$$

$$\frac{r_{a2}r_{a3}\left(\frac{f_a}{1-f_a}\right)\left(\frac{f_b}{f_c}+1\right)+r_{a3}\left(\frac{f_b}{f_c}\right)+r_{a2}}{r_{a2}r_{a3}\left(\frac{f_a}{1-f_a}\right)\left(\frac{f_b}{f_c}+1\right)+2\left[r_{a3}\left(\frac{f_b}{f_c}\right)+r_{a2}\right]} \quad (21)$$

The conversion from monomer to structural units implicates reaction transformation more beyond the conversion rate. The tercopolymerization scheme can tell not just the isocyanate and hydroxyl structural distribution but more about urethane and urea repeat units influence and changes over reactions. The instantaneous tercopolymer composition was defined as $Y_a + Y_b + Y_c = 1$. To identify the relations of structural units composition, the aspect ratio of two mole fractions in the polymer at the instant times B and C can be evaluated:

$$\frac{Y_b}{Y_c} = \frac{d[B]}{d[C]} = \frac{k_{12}[B]}{k_{13}[C]} = \frac{k_{12}f_b}{k_{13}f_c} = \frac{k_{12}k_{11}f_b}{k_{13}k_{11}f_c} = \frac{r_{a3}f_b}{r_{a2}f_c} \quad (22)$$

Then:

$$\frac{f_b}{f_c} = \frac{r_{a2}Y_b}{r_{a3}Y_c} \quad (23)$$

Thus the instantaneous tercopolymer composition equation becomes:

$$Y_a = \frac{r_{a2}r_{a3}\left(\frac{f_a}{1-f_a}\right)\left(\frac{f_b}{f_c}+1\right)+r_{a3}\left(\frac{f_b}{f_c}\right)+r_{a2}}{r_{a2}r_{a3}\left(\frac{f_a}{1-f_a}\right)\left(\frac{f_b}{f_c}+1\right)+2\left[r_{a3}\left(\frac{f_b}{f_c}\right)+r_{a2}\right]} =$$

$$\frac{r_{a2}r_{a3}\left(\frac{f_a}{1-f_a}\right)\left(\frac{r_{a2}Y_b}{r_{a3}Y_c}+1\right)+r_{a3}\left(\frac{r_{a2}Y_b}{r_{a3}Y_c}\right)+r_{a2}}{r_{a2}r_{a3}\left(\frac{f_a}{1-f_a}\right)\left(\frac{r_{a2}Y_b}{r_{a3}Y_c}+1\right)+2\left[r_{a3}\left(\frac{r_{a2}Y_b}{r_{a3}Y_c}\right)+r_{a2}\right]} =$$

$$\frac{\left(\frac{f_a}{1-f_a}\right)\left[r_{a2}\left(\frac{Y_b}{Y_c}\right)+r_{a3}\right]+\frac{Y_b}{Y_c}+1}{\left(\frac{f_a}{1-f_a}\right)\left[r_{a2}\left(\frac{Y_b}{Y_c}\right)+r_{a3}\right]+2\left[\frac{Y_b}{Y_c}+1\right]} \quad (24)$$

Where $\frac{f_a}{1-f_a}$ denotes the mole fraction ratio of isocyanate and hydroxyl groups including water in the feed at the same instant time, $\frac{Y_b}{Y_c}$ denotes the mole fraction ratio of urethane and urea linkages in hard segments. The reactivity ratios can be calculable based on scenarios.

The empirical kinetic reaction constant of isocyanate trimerization was calculated from measured reaction parameters under catalyzed condition [15]. The rate constant k_{11} is derived from generalized 3rd order reactions:

$$-\frac{d[A]}{dt} = \frac{d[A_t]}{dt} = 3k_{11}[A]^3 \quad (25)$$

Where $[A_t]$ is the isoscyante trimerization concentration. The derived value is $k_{11} = 20.5 \times 10^{-4}$ ($dm^3mol^{-1}s^{-1}$) at DABCO catalyzed condition with temperature 60°C [16, 17].

Bifunctional Reactions

Diol and diisocyanate reaction is the preliminary conditional setup for kinetic scheme, the rate constants for reactivity calculation are obtainable from experimental measurements [16, 17]. As measured, the reaction rate of DABCO catalyzed reaction between 2,4-TDI and 1,4-butanediol at condition with temperature 60°C is $k_{12} = 68.1 \times 10^{-4}$ ($dm^3mol^{-1}s^{-1}$). The relative reactivity of hydroxyl and water is almost the same, so k_{13} is defined at the same value as k_{12} [18]. Thus the reactivity ratios are derived, $r_{a2} = r_{a3} = 0.30$. The instantaneous tercopolymer composition equation becomes:

$$Y_a = \frac{0.3\left(\frac{f_a}{1-f_a}\right)+1}{0.3\left(\frac{f_a}{1-f_a}\right)+2} \quad (26)$$

Macropolyol Reactions

In most applied industrial cases, diisocyanate prepolymer reacts with macropolyol to form crosslinked polymer. Here the polymerization condition was assumed to occur between commonly used TDI blends (2,4/2,6 isomer ratio = 65/35) and polyethylene-propylene glycols (primary/secondary hydroxyl ratio = 70/30) [4]. The relative reactivity of 2,4-TDI and 2,6-TDI sets to 2.1 [19] and that of primary and secondary hydroxyl groups sets to 3.3 [18]. Thus the reactivity ratios were derived:

$$r_{a2} = \frac{k_{11}}{k_{12}} = \frac{(20.5\times10^{-4})\times65\% + \left(\frac{20.5\times10^{-4}}{2.1}\right)\times35\%}{68.1\times10^{-4}\times70\% + \left(\frac{68.1\times10^{-4}}{3.3}\right)\times30\%} = 0.31 \quad (27)$$

$$r_{a3} = \frac{k_{11}}{k_{13}} = \frac{(20.5\times10^{-4})\times65\% + \left(\frac{20.5\times10^{-4}}{2.1}\right)\times35\%}{68.1\times10^{-4}} = 0.25 \quad (28)$$

So the instantaneous tercopolymer composition equation becomes:

$$Y_a = \frac{\left(\frac{f_a}{1-f_a}\right)\left[0.31\left(\frac{Y_b}{Y_c}\right)+0.25\right]+\frac{Y_b}{Y_c}+1}{\left(\frac{f_a}{1-f_a}\right)\left[0.31\left(\frac{Y_b}{Y_c}\right)+0.25\right]+2\left[\frac{Y_b}{Y_c}+1\right]} \quad (29)$$

Structural Units Effect

The analysis of constitutional repeating structural units can tell the conversion mechanism of monomers. In polyurethane chemistry, two linkages of urethane and urea are major repeating units with certain fixed molecular structure. The isocyanurate structure is more presented at isocyanate excessive condition. The isocyanate conversion rate, structural unit formation, and units sequence distribution are all together in certain proportion with mole fractions in formulation. In this study, the ratio comparison method was employed to investigate the influence of structural unit difference on isocyanate conversion and urethane and urea formation.

$\frac{f_a}{1-f_a}$ can represent any possible unit structural arrangements or some units other than urethane or urea formation in circumstance. $\frac{Y_b}{Y_c}$ can tell any arrangement disproportionateness induced structural irregularity. The comparisons of these two were charted in **Figure 1**.

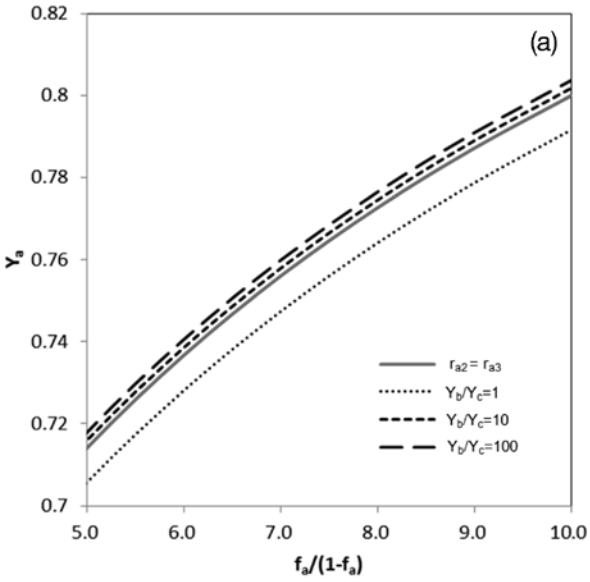

***Figure 1**. Mole ratio comparison of structural units changes*

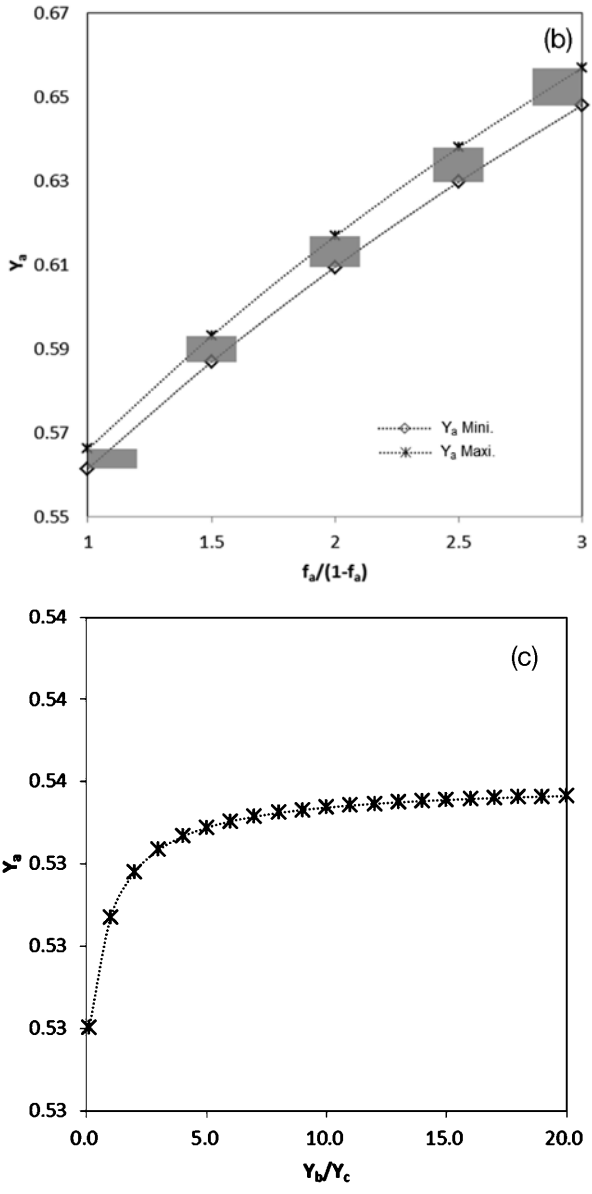

***Figure 1**. (Cont'd...) Mole ratio comparison of structural units changes*

Figure 1a implicates the ratio impact of hydroxyl/water structural units on isocyanate conversion. No pronounced influence was observed in conversion comparison, but when the urethane linkage content far overperforms urea $(\frac{Y_b}{Y_c} \gg 1)$ in absence of water the isocyanate conversion can be elevated which

suggests water can improve hardness by forming urea hard block and also impact on isocyanate conversion to some extent. The bifunctional reaction (r_{a2}=r_{a3}) was also presented in contrast which reflects the conversion rate of bifunctional reaction is comparable with macropolyol reaction in catalyzed condition. **Figure 1b** presents the urethane and urea units ratio changes $\frac{Y_b}{Y_c}$ (solid black bar) over mole ratio change of isocyanate and polyols $\frac{f_a}{1-f_a}$. In the iso/polyol mole ratio range 0.5~3, the isocyanate structural unit was promoted which indicates remaining unreacted isocyanate existing resulted from high concentration. The increasing bar length of $\frac{Y_b}{Y_c}$ over iso/polyol ratio indicates that the formed urethane/urea sequence goes together with isocyanate unit in correlating proportion. The conclusion can be drawn that high ratio of urethane over urea in sequence resulting from increasing isocyanate amount can possibly further promote isocyanate conversion. **Figure 1c** exhibits the relation between structure units (Y_a, Y_b, Y_c). The instantaneous isocyanate structural unit presents extremely low in urea dominated hard phase sequence which confirmed higher reactivity of water producing more urea linkage at initiation. It also suggests the sequence composition may have impact on isocyanate conversion rate. This circumstance can be rationalized by better thermodynamic stability of urethane over urea owing to stabilization of carboxylate structure resonance delocalizing the nitrogen atom.

CELL CONFIGURATION MECHANISM

Reactivity Profile

Cell configuration in polyurethanization is a time-dependant process of producing bubbles under irreversible synergetic efforts of shear force, viscoelasticity, vapor pressurization, and Gibbs free energy. The measurements of foaming process are technically challenging because of the out-of-equilibrium heterogeneity. But the commercially available FOAMAT reactivity profiling software makes it more accessible by monitoring the entire foaming process with time-scale recording [20]. The recorded reaction parameters include foam rise, reaction temperature, foaming pressure, polymerization rate, viscosity change, and curing time. The non-equilibrium polymerization over time between polyol and isocyanate under additives synergetic effects can be characterized by these variables.

Foam Rise

Foam rise height is evidently one of the primary reactivity factors. Blowing agents vaporization heated by exothermal reactions elevates the cell gaseous pressure. The produced highly porous polymers can be characterized by relative density $(\frac{\rho^*}{\rho})$ [21] and foam porosity $(1-\frac{\rho^*}{\rho})$ [22]. The foam rise $H(t)$ resulting from cell configuration is a dynamic combination of polymer solidification and gaseous blowing which can be mathematically characterized into formula:

$$H(t) = H_c = H_p + H_g \tag{30}$$

Meanwhile, the foam volume $V(h)$ can be defined as total cell volume V_c, a combination of polymer volume V_p and gaseous volume V_g:

$$V(h) = V_c = V_p + V_g \tag{31}$$

Reaction Temperature

Temperature dynamics reflect the entire polymerization progress. The maximum temperature represents reaction completion. Temperature ascendance is practically governed by kinetic reaction rates of catalyzed polymerization. The catalyzation accelerates polyaddition and oligomerization and meanwhile drives up the temperature. On the contrary, the temperature acceleration implicates ongoing catalyzation. The temperature increase usually decelerates at threshold gel time (GT) and turns around into decrease after complete cure at tack free time (TFT) in **Figure 2**. Some catalysts such as dibutyltin dilaurate (DBTDL) and blocked catalysts can extend the reaction time resulting in slow temperature rise and stretching curing time.

Foaming Pressure

Foam pressure is measurable (**Figure 3**) and calculable from mole weighted vapor pressure of cell gas mixture at certain temperature, the data of which may differs on chosen blowing agents and can be escalated with more catalyst presence. Blowing agents vaporization helps realize more cell coarsening. The gas diffusion and heat transfer between cells aggravate pressure growth. The relationship between measured pressure in FOAMAT and weight parts of blowing agents in formulation can be expressed in formula:

$$P(t) = \sum_{i=1}^{n} f_i P_i + f_{CO_2} P_{CO_2} + f_{air} P_{air} \tag{32}$$

$$f_i = \frac{n_i}{n_{tot}} \tag{33}$$

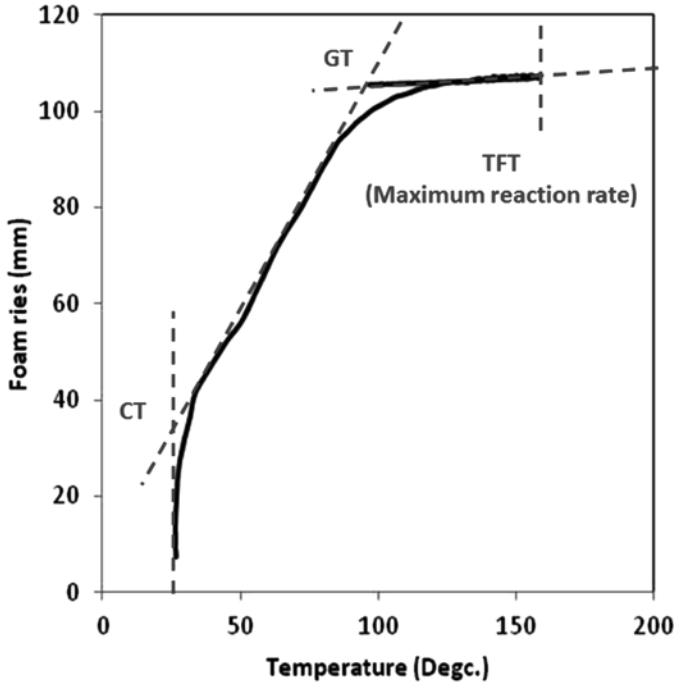

***Figure 2**. Polyisocyanurate foam rise over temperature (Baydur sample FOAMAT tests)*

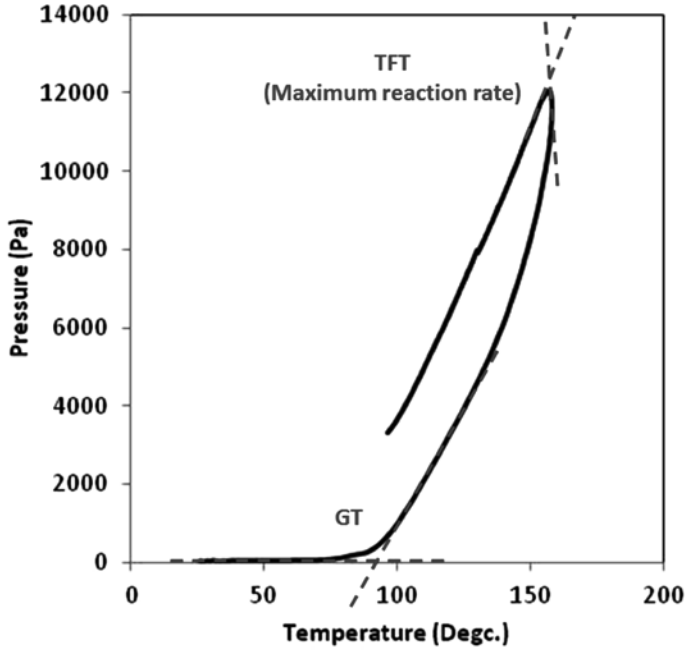

***Figure 3**. Polyisocyanurate pressure over temperature (Baydur sample by FOAMAT tests)*

where f_i and P_i are mole fraction and vapor pressure of defined blowing agent. The formula also includes fractionated carbon dioxide and air vapour pressures. The mole fractions are derivable from experimental measurements or empirical estimation. The amount of blowing agent is obtainable from formulation. The vapor pressure P_i can be collected from publically available thermophysical properties tables. The measured pressure changes proportionate to temperature changes in terms of the ideal gas law $\left(R = \frac{PV}{nT}\right)$, from which the dynamic changes of gas volume V_g can be calculated.

Polymerization Rate

The polyurethane reaction kinetics can be modelled [3, 23] by reaction progress monitoring and mathematically manipulated by reaction differentiation or integration as follows:

$$\frac{d[PU]}{dt} = K[Pol][Iso] \tag{34}$$

Where K is the reaction rate coefficient of polyurethane, specifically for PUR when equivalent weight of polyol and isocyanate is same, then:

$$\frac{d[PU]}{dt} = \frac{d[PUR]}{dt} \tag{35}$$

but for PIR when the index is higher and isocyanate amount presents over polyol resulting in trimerization, then:

$$\frac{d[PU]}{dt} = \frac{d([PUR]+[PIR])}{dt} \tag{36}$$

FOAMAT defines reaction rate by unit time foam rise which is practically easy to measurement but scientifically bias in definition, because foam rise height is more attributable to blowing agent functioning and less effective to chemical polymerization. More accuracy can be achieved by measuring temperature rise in unit time which can synchronize heat release with corresponding reaction progress and mitigate the misleading accounts of physical blowing effect of blowing agents. Moreover, FOAMAT default setting of gel time (GT) is 15% foaming pressure rise and for curing time is 10% dielectric polarization rise that also mistakes reactivity determination by mixing factor of blowing agents causing variability in both measurements. The developed tangent line analysis method can significantly improve the measurement accurateness based on currently collected reaction rate curves from FOAMAT (**Figure 4**). The sample rigid foam reaction rate graph presents sharp hill growth from baseline. Cream

time (CT), gel time (GT), and tack free time (TFT) are suggested to define as the intersection of tangent line with baseline in respective ascending, descending, and flat domains.

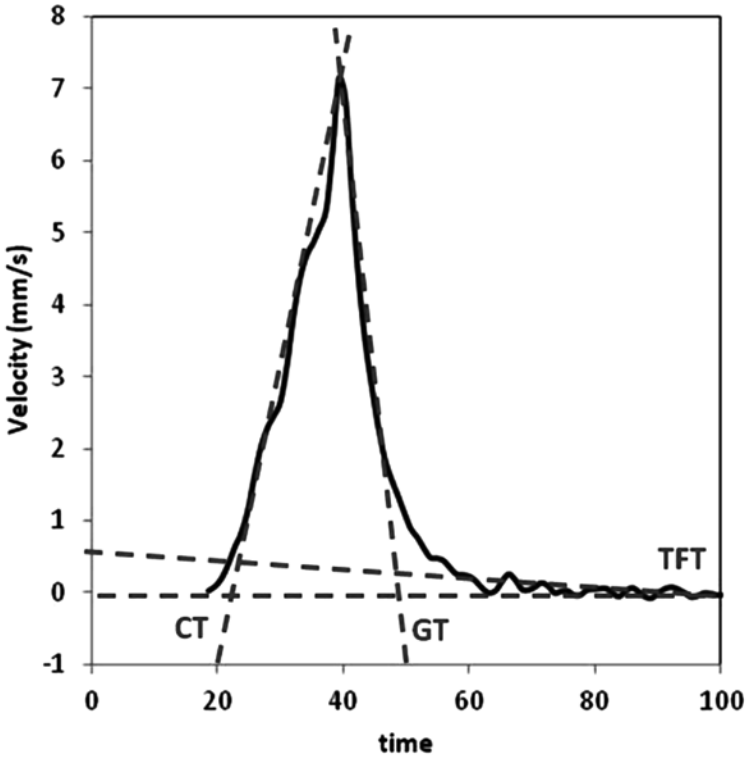

***Figure 4**. Reactivity time definition (Baydur sample FOAMAT tests)*

Viscosity Changes

Viscosity features the polyurethane reaction in liquid-solid state equilibrium. The sharp "U-turn" graph (**Figure 5**) over the polymerization process implicates that the viscosity growth initiates at cream time (CT), reduces deeply with the exothermal reaction acceleration, it touches down the minimum bottom when is the defined watershed time between primary reactions and secondary reactions, and then undertakes sharp rise with more crosslinking till the end at gel time (GT). As observed on the same profile, this dynamic growth is in pair with reaction rate changes.

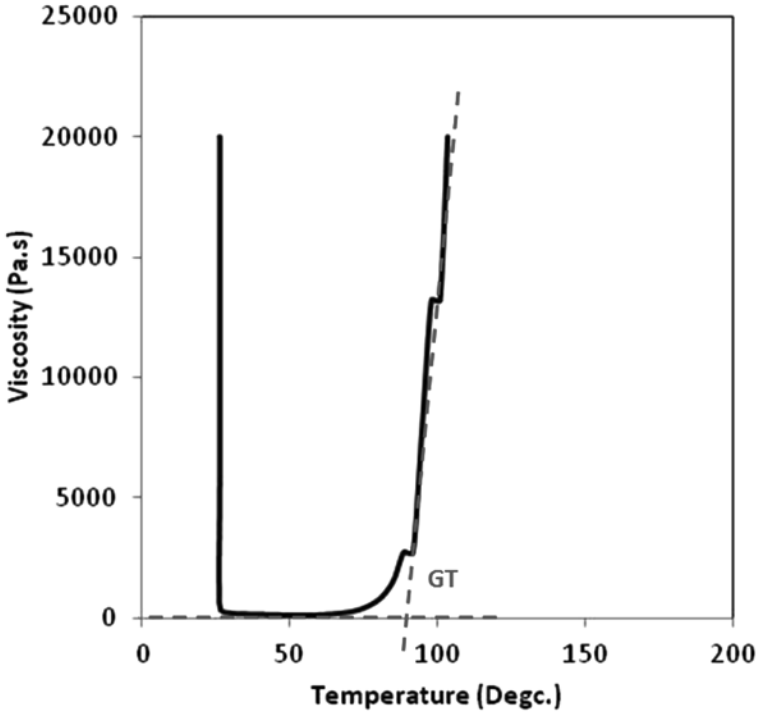

***Figure 5**. Polyisocyanurate viscosity over temperature (Baydur sample FOAMAT tests)*

Curing Time

Dielectric polarization is rarely measured feature to characterize the polyurethane curing process based on electrochemical mechanism. The dielectricity is generated by polarized groups (-OH and –NCO) with large dipole moment. The electromagnetic vibration starts when reaction begins, continues during polymerization, and eventually calms dawn gradually after maximum reaction threshold passed when the dipole mobility is suppressed by crosslinking and solidification and turns into zero till liquid-solid state equilibrium [24, 25].

Cell Configuration Modelling

The foam cell microstructure configuration can be progressively monitored by in-suite optical instruments but needs more meticulous analytic skills. The sophisticated cell construction software i.e. Surface Evolver can make great computational simulation for microstructural and microgeomeric study. Such

computational efforts can provide cell morphology visualization and essential voxel data to facilitate structure characterization and micromechanical modelling. Nonetheless, the generalized theoretical modelling by combination of foaming reactivity and cell configuration in this study can provide more insight of cell growth evolvement in physic chemistry significance.

In this study the cell microstructure configuration model was developed based on FOAMAT reactivity profile. The measured parameters are transferred and consolidated into easily accessible correlation for modeling. $H(t)$, $P(t)$, $r(t)$, $\mu(t)$, $m(t)$ respectively denote foam rise, gaseous vapor pressure, polymerization reaction rate, foam viscosity, and foam weight. The polyurethane foam was hypothesized as bulk microporous solid composed of infinite uniform unit cells in number of (n+1) and each unit cell is microgeometrically idealized into sphere with radius and corresponding surface area $A_0 = 4\pi r^2$ and volume $V_0 = \frac{4}{3}\pi r^3$. Thus the total foam volume can be defined as volumetric sum of individual cell $V_c = (n + 1)V_0$. The same logics for total surface area $S_c = (n + 1)S_0$. Thus the ratio relationship between cell surface and cell volume becomes:

$$\frac{S_c}{V_c} = \frac{(n+1)S_0}{(n+1)V_0} = \frac{A_0}{V_0} = \frac{4\pi r^2}{\frac{4}{3}\pi r^3} = \frac{3}{r} \tag{37}$$

Where S_c is calculable from measured $V(t) = V_c$ if is derived.

The interstitial border area of two unit cells is approximated into sandwich combination of two gas-solid interfaces and one cell strut between two cell gas phases (**Figure 6**).

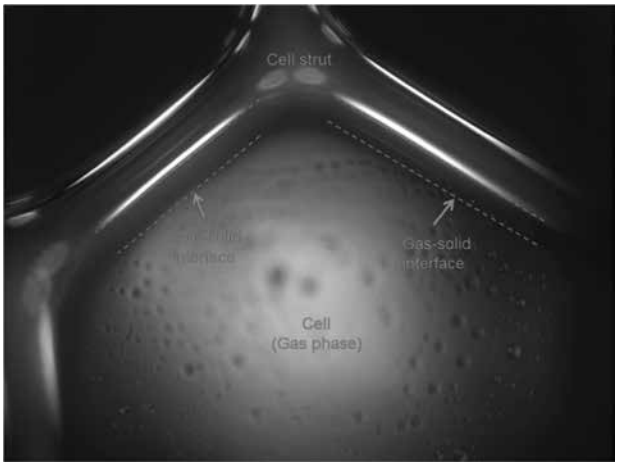

***Figure 6**. Interstitial border area between cells*

The thickness of interstitial border t_c is defined as:

$$t_c = t_s + t_w \tag{38}$$

Where t_s denotes unit strut mid-section thickness and t_f denotes unit cell wall thickness. Under magnitude gas vapor pressure $P(t)$ on assumed edge area A resulting from polymerization heat release, the proportional foam rise speed $r(t) = \frac{dH(t)}{dt}$ as defined by FOAMAT foam rise rate. The polymer viscosity $\mu(t)$generates by this force acting as shear stress over perpendicular gradient $\frac{\partial r(t)}{\partial y}$ can be expressed as follows:

$$\mu(t) = \frac{P(t)}{r(t)}\frac{y}{A} \tag{39}$$

From general linear correlation of shear velocity and gradient, the interstitial border volume was assumed as the total cell solid volume $V_p = Ay$, $A = n\left(\frac{\pi}{4}t_c^2\right)$ and $H_p = nt_c$. Further the XZ cross-section area of which (**Figure 5**) can be assumed as the area under shear velocity curve and expressed as follows:

$$\int r(t)dy = \int \frac{P(t)}{\mu(t)}\frac{y}{A}dy = \int \frac{P(t)V_p}{\mu(t)A^2}dy = \frac{y}{2}\frac{P(t)V_p}{\mu(t)A^2} = nt_c y \tag{40}$$

Then t_c^2 can be obtained:

$$t_c^2 = \frac{16P(t)V_p}{2\mu(t)\pi^2 H_p^3} \tag{41}$$

H_p can be calculable from foam rise $H(t)$ multiplied by gas/solid volumetric fraction coefficient $x = \frac{H_p}{H_c} = \frac{V_p}{V_c}$ or mole fraction $x = \frac{n_p}{n_c}$ which can be approximated and simplified to obtain from measured partial pressure $P(t)$ devided by saturated vapor pressure P_o, $1 - x = \frac{P(t)}{P_0}$. Alternatively it can be derived from product concentration [*PU*] calculated from simplified polyurethane kinetic model:

$$[PU] = [PUR] = [Pol]_0\left(1 - e^{-\frac{K_u}{K_i}[Iso]_0\left(1-e^{-K_i t}\right)}\right) \tag{42}$$

$$[PU] = [PUR] + [PIR] = [Pol]_0\left(1 - e^{-\frac{K_u}{K_i}[Iso]_0\left(1-e^{-K_i t}\right)}\right) + [Iso]_0(1 - e^{-K_i t}) \tag{43}$$

Where K_u and K_i are kinetic constants of polyurethane stepwise reaction – isocyanate polyaddition and oligomerization (trimerization). Thus, the interstitial border thickness is expressed:

$$t_c = \sqrt{\frac{8P(t)V_p}{\pi^2\mu(t)H_p^3}} = \sqrt{\frac{8P(t)V(t,x)}{\pi^2\mu(t)H(t,x)}} = \sqrt{\frac{8P(t)V(t)}{\pi^2\mu(t)H(t)}} \tag{44}$$

The foam rise $H(t)$ which is a combination of gas and solid heights can be anatomically characterized by integration:

$$H(t) = H_p + H_g = nt_c + 2(n+1)r \tag{45}$$

So the unit cell radius can be obtained by following formula:

$$r = \frac{H_g}{2(n+1)} = \frac{(1-x)}{2(n+1)}H(t) \tag{46}$$

Where $n = \frac{H_p}{t_c} = \frac{x}{t_c}H(t)$.

The cell growth starting from nucleation to propagation is governed by surface tension and vapor pressure. The cells with curved liquid/vapor interface with radius r are growing under thermodynamic principles. Kelvin equation which describes the change in vapor pressure in interface at equilibrium condition can also be used to determine the cell porosity and configuration progress. Thus the dynamic interface energy density γ can be defined as a combination of gas surface tension γ_g and polymer surface tension γ_p:

$$\gamma = \gamma_g - \gamma_p \tag{47}$$

With reaction temperature increase, γ_g is getting larger than γ_p, when $\gamma > 0$, the Gibbs free energy grows up and the cell size starts inflation after nucleation driven by released heat. Open cell foam creates when surfactant surface tension cannot over-perform cell partial pressure or closed cell foam creates when surfactant successfully contains cell dilation and the surface tension reaches equilibrium at $\gamma = 0$. The gas and polymer surface tensions γ_g and γ_p can be obtained through evaluation:

$$\gamma_g = \frac{rRT}{2V_g}\left(ln\frac{P(t)}{P_0}\right) = \frac{ln(1-x)rRT}{2(1-x)V(t)} \tag{48}$$

$$\gamma_p = \frac{rRT}{2V_p}\left(lnC_p\right) = \frac{ln(x)rRT}{2xV(t)} \tag{49}$$

Where C_p is polymer concentration, R is universal gas constant, and T is temperature.

The dynamic changes of surface tension was assumed as a non-equilibrium surface tension evolvement (Υ) = $\int\gamma(t)dt$ over time period composed of infinitesimal change dt of interface equilibrium at time t with initial equilibrium boundary condition of cell nucleation at $\gamma_0 = 0$ and close equilibrium boundary condition of cell stabilization at $\gamma_t = 0$. Thus, at infinitesimal equilibrium the total sum of gas and polymer chemical potentials is zero as free energy is at minimum, so:

$$d\mu_g + d\mu_p = 0 \tag{50}$$

Which is substituted into Gibbs absorption equation:

$$-d\gamma = \Gamma_g d\mu_g + \Gamma_p d\mu_p \tag{51}$$

$$-\frac{d\gamma}{d\mu_p} = \Gamma_p - \Gamma_g \tag{52}$$

Where Γ_g and Γ_p are gas and polymer surface excess which represent unit gas/polymer molecules accommodation in interface. The interface inhomogeneity governs the surface excess, it varies gradually over the interfacial region attributable to the concentrations of both components which are liquid blowing agents and polyol-isocyanate mixture with complete dilution and perfect dispersion. The equilibrium breaks up with temperature rise during which the blowing agents physical vaporization complicates the process by contact phase change. Further, the surface excess dynamic evolvement is factored by contact surface tension and gas/liquid/solid polymer concentration changes. Through the evaluation of chemical potential equation by differentiation, the gas and polymer surface excess formula in Gibbs isotherm can be obtained:

$$\Gamma_g = -\frac{1}{RT}\frac{d\gamma_g}{dlnC_g} \tag{53}$$

$$\Gamma_p = -\frac{1}{RT}\frac{d\gamma_p}{dlnC_p} \tag{54}$$

Then Gibbs absorption equation can be re-evaluated:

$$-\frac{d\gamma}{d\mu_p} = \Gamma_p - \Gamma_g = -\frac{1}{RT}\left(\frac{d\gamma_p}{dlnC_p} - \frac{d\gamma_g}{dlnC_g}\right) \tag{55}$$

$$\Gamma = \Gamma_{\mathrm{p}} - \Gamma_{\mathrm{g}} \tag{56}$$

Where Γ is defined as total surface excess at interface, a combination of gas surface excess Γ_{g} and polymer surface excess Γ_{p}. $\Gamma = 0$ in idealized model and $\Gamma > 0$ in real phases. As polymerization undergoing, gas surface excess Γ_g is getting smaller and $\Gamma_g \approx 0$ and $\Gamma \approx \Gamma_p$ when polymer completely cures. Under complete cure state at equilibrium $\gamma_t = 0$, total surface excess Γ denoting polymer mole quantity on unit dividing surface area can be calculated:

$$\Gamma \approx \Gamma_{\mathrm{p}} = \frac{n_w}{S_c} = \frac{n_p - n_s}{S_c} \tag{57}$$

Where n_w are moles of polymer at cell wall, n_p are total moles of polymer in foam, and n_s are moles of cell strut. S denotes the total surface area of cells in foam. The interfacial region varies gradually during foaming because of the concentration changes and regional distance between two bulks – cell gas mixture and crosslinked polymer – is creating which ultimately cures into cell wall. The cell wall thickness is calculable by follows:

$$\Gamma = \frac{n_w}{S_c} = \frac{n_w t_w}{V_w} = \frac{m_w t_w}{M_w V_w} = \frac{\rho_w t_w}{M_w} = \frac{\rho_p t_w}{M_p} \tag{58}$$

$$t_w = \frac{\Gamma M_p}{\rho_p} = \frac{xV(t)}{m(t)} \Gamma M_p \tag{59}$$

The cell strut density ρ_{w} and molecular weight M_{w} were assumed unitary as polymer data, $\rho_{\mathrm{w}} = \rho_{\mathrm{p}}$, $M_{\mathrm{w}} = M_p$. The polymer density ρ_{p} is calculable from FOMAT measurements, $\rho_p = \frac{m(t)}{xV(t)}$. The polymer molecular weight M_p is partial molecular weight of formulation derived from fractional equation evaluation.

Macroscopic anisotropy can be observed in rigid foam production by continuous line. The three dimensional compress strength measurements present large difference at axis across panel thickness which is much smaller than the values of other two which indicates the close-to-sphere cell microgeometry of a large number of cells are not the case anymore which is replaced by elongated or flattened close-to-ellipsoid shape. The line speed may aggravate the result to some extent. This cell microscopic orientation in preferred direction is the common cause for anisotropy and even slight elongation can produce large difference in properties. Cell anisotropic degree R_a is an aspect ratio of the largest and smallest principal cell dimensions. The continuous line production donates shear stress to cell growth through

inertial force from line speed which produces tensile strength in X-direction that performs as joint surface force in tandem with partial pressure of cell gas mixture which also results in cell surface tension during cell inflation to generate cell anisotropy.

The hypothesis conditions that unit cell with uniform density deforms from sphere with volume V_0 and radius r to spheroid with volume V'_0 a pair of equal semi-axes a at Y and Z and a distinct third semi-axis b at X which is the only direction under shear stress effect. The volume formula of spheroid is:

$$V_0^{'} = \frac{4}{3}\pi a^2 b \tag{60}$$

Where $a = r$ and $r = \left(\frac{3V_0}{4\pi}\right)^{\frac{1}{3}}$, and so cell anisotropic degree R_a can be calculated:

$$R_a = \frac{b}{a} = \frac{V_0^{'}}{V_0} = \frac{V(t)^{'}}{V(t)} \tag{61}$$

The hypothesis for the cells number in equilibrium is that both are the same in two assumed measurements of both homogeneity and inhomogeneity and further differentiations of both demonstrate the same relationship of infinitesimal volumes:

$$R_a = \frac{db}{da} = \frac{dV_0^{'}}{dV_0} = \frac{\partial V(t)^{'}}{\partial V(t)} \tag{62}$$

As hypothesis of two shapes of cells – sphere and spheroid – with uniform density and equilibrated foaming condition (**Figure 7**), the surface energy produced from cell inflation by vapor pressure are same, $W = PdV = P'_0 dV'$. Thus the following surface working energy relationship can be easily found:

$$PdV = P_0^{'}\, dV^{'} = \left[P\cos\left(\frac{\pi}{2} - \theta\right) + (P + \tau)\cos\theta\right] dV^{'} \tag{63}$$

The shear velocity can be derived $dv = \frac{db}{t}$ as assumed local shear deformation at X-axis along the extension distance b. The local movement at Y-axis with distance $da = dy$. Thus the viscous force τ becomes:

$$\tau = \frac{\mu}{t}\frac{db}{da} \tag{64}$$

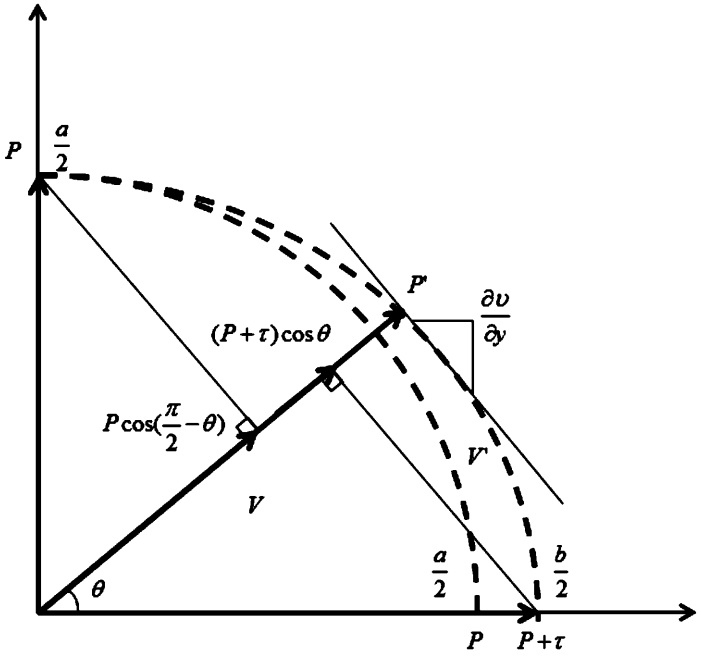

***Figure 7**. Pressure analysis of cell elongation*

Thus cell anisotropic degree R_a can be obtained from evaluation on the surface working energy relationship between two assumed cell inflation growths Eq (63):

$$R_a = \frac{1-\frac{\mu}{Pt}cos\theta}{sin\theta+cos\theta} \tag{65}$$

Where angle θ is defined shear deformation degree, $\theta = \cot^{-1}\frac{\partial v}{\partial y}$. The relationship between viscosity μ, pressure *P*, and cell anisotropic degree R_a can be derived as follows through further evaluation which implicates the strong functions of pressure and viscosity on cell orientation.

$$R_a = \frac{1-\frac{cos\theta d\mu}{P\ \ dt}}{sin\theta+cos\theta} \tag{66}$$

$$\mu = \frac{1}{cos\theta}\int P[1 - R_a(sin\theta + cos\theta)]dt \tag{67}$$

In interface equilibrium of elongated cells:

$$P_0^{'}\ \frac{dV}{dt} = \gamma_0^{'}\ \frac{dS}{dt} \tag{68}$$

The volume and surface area are given simply in terms of elementary functions:

$$V = V_0^{'} = \frac{4}{3}\pi a^2 b = \frac{4}{3}\pi b^3(1-e^2) \tag{69}$$

$$S = S_0^{'} = 2\pi a^2\left(1+\frac{b}{ae}\sin^{-1}e\right) \tag{70}$$

And then the differentiation relationship can be derived:

$$dV = \frac{4}{3}\pi b^3(1-e^2)de = -\frac{8}{3}\pi b^3 ede \tag{71}$$

$$dS = 2\pi a^2\left(1+\frac{b}{ae}\sin^{-1}e\right)de = \frac{2\pi a^2 b}{ae}(\sin^{-1}e)de = \frac{2\pi a^2 b}{e}\left(\frac{1}{\sqrt{1-e^2}}-\frac{\sin^{-1}e}{e}\right)de \tag{72}$$

Thus the relationship between pressure and surface tension can be found:

$$\frac{P_0^{'}}{\gamma_0^{'}} = \frac{dS}{dV} = \frac{\frac{2\pi a^2 b}{e}\left(\frac{1}{\sqrt{1-e^2}}-\frac{\sin^{-1}e}{e}\right)}{-\frac{8}{3}\pi b^3 e} = \frac{3a^2}{4b^2e^2}\left(\frac{\sin^{-1}e}{e}-\frac{1}{\sqrt{1-e^2}}\right) \tag{73}$$

Where unit cell pressure and surface tension is assumed the same as bulk measurement $P(t)$ and derived $\gamma(t)$.

CONCLUSIONS

The sequence arrangements of polyisocyanurate chains were analysed by polymer statistics. PIR/PUR ratio was developed based on generalized two steps copolymerization of hydroxyl-isocyanate urethanization and isocyanate homocyclization. The evaluation of Mayo-Lewise tercopolymerization kinetic scheme suggests the isocyanurate structural units formation is manipulated by two factors of isocyanate concentration and formed urethane/urea ratio, and the isocyanurate structure has little impact on isocyanate conversion rate

even in higher excess amount. This structural stabilization is increasing with more urethane linkage formation. Moreover, the developed cell microstructure growth model from interstitial border and Gibbs absorption analysis further provided a localized characterization of individual cell construction during foaming which also developed a practical solution to cell anisotropic degree calculation.

ACKNOWLEDGEMENTS

This work was supported by the NSFC (Grant No. 21403119). The authors would like to thank the kind assistance offered by the Honeywell Shanghai Lab team for experimental support of FOAMAT profiling.

REFERENCES

1. Kaushiva B.D., Ph.D. dissertation, Virginia Polytechnic Institute (1999).
2. Efstathiou K., BME report, Budapest University of Technology and Economics (BME) (1999).
3. Edelmann M., Gedan-Smolka M., Lehmann D., *Prog. Org. Coat*. **57** (2006), 251-258.
4. Randall D., Lee S., The Polyurethanes Book, John Wiley & Sons (2002), 113-126.
5. Burns S.B., Schmidt E.L., *J. Cell. Plas*., **29** (1993), 437-438.
6. Jacobson H., Stockmayer W.H., *J. Chem. Phys*., **18** (1950), 1600-1606.
7. Semlyen J.A., Large Ring Molecules, Wiley (1996).
8. Baser S.A., Khakhar D.V., *Polym. Eng. Sci*., **34** (1994), 642-649.
9. Haberstroh E., Zabold J., *J. Polym. Eng*., **24** (2004), 377-390.
10. Seo D., Youn J.R., *Polym.*, **46** (2005), 6482-6493.
11. Mao D., Harvey A.D., Edwards J.R., *WIT Trans. Eng. Sci*., **20** (2005), 327.
12. Geier S., Winkler C., Piesche M., *Chem. Eng. Tech*., **32** (2009), 1438-1447.
13. Bikard J., Bruchon J., Coupez T., Silva L., *Coll. Surf. A: Phys. Eng. Asp*., **309** (2007), 49-63.
14. Bikard J., Bruchon J., Coupez T., Vergnes B., *J. Mat. Sci*., **40** (2005), 5875-5881.

15. Viola G.G., Schmeal W.R., ***Polym. Eng. Sci***., **34** (1994), 1173-1186.

16. Krol P., ***J. Appl. Polym. Sci***., **57** (1995), 739-749.

17. Krol P., Atamanczuk B., Pielichowski J., ***J. Appl. Polym. Sci***., **46** (1992), 2139-2146.

18. Ghoreishi R.Y., Zhao S., Suppes G.J., ***J. Appl. Polym. Sci.***, **131** (2014), 469-474.

19. Odian G., Principles of Polymerization, John Wiley & Sons, Inc. (2004).

20. Gibson L.J., Cellular solids: Structure and properties, 2nd ed, Cambridge University Press, Cambridge (1997).

21. Foam qualification system FOAMAT: Measuring physical parameters during foam formation, Foamat Messtechnik GmbH (1999).

22. Placido E., Arduini-Schuster M.C., Kuhn J., ***Infr. Phys. Tech.***, **46** (2005), 219.

23. Lapprand A., Boisson F., Delolme F., Mechin F., Pascault J.P., ***Polym. Degr. Stab.***, **90** (2005), 363-373.

24. Kao K.C., Dielectric phenomena in solid, Academic Press (2004).

25. Kasap S., Principles of electronic materials and device, 3rd ed., McGraw-Hill (2006).